Available online at www.sciencedirect.com
ScienceDirect
ELSEVIER
Gondwana Research xx (2007) xxx–xxx
INTERNATIONAL ASSOCIATION FOR GONDWANA RESEARCH GR
www.elsevier.com/locate/gr

Foreland basin deposits associated with Cuyania accretion in La Pampa Province, Argentina

Carlos J. Chernicoff [a,b,*], Eduardo O. Zappettini [b], João O.S. Santos [c,d], Eloise Beyer [e], Neal J. McNaughton [c]

[a] *Council for Scientific and Technical Research (CONICET), Julio A. Roca 651, 1322 Buenos Aires, Argentina*
[b] *Argentine Geological-Mining Survey (SEGEMAR), Julio A. Roca 651, 1322, Buenos Aires, Argentina*
[c] *University of Western Australia, 35 Stirling Highway, 6009 Perth, Australia*
[d] *Redstone Resources, 110–116 East Parade, 6004 Perth, Australia*
[e] *GEMOC, Department of Earth and Planetary Sciences, Macquarie University, Herring Road, North Ryde, Sydney, NSW 2109, Australia*

Received 13 March 2007; received in revised form 10 April 2007; accepted 16 April 2007

Abstract

In the province of La Pampa, south-central Argentina, adjacent to the Cuyania–Pampia terrane boundary, a Late Ordovician–Devonian marine foreland basin generated after the Middle Ordovician (Darriwilian) collision of Cuyania has been recognised, and is herein referred to as the Curacó basin. This basin was formed on crust of the Cuyania terrane, immediately to the west of the Pampia terrane. Its fill primarily comprises sandstones and shales of the La Horqueta Formation, unconformably overlain by Permian continental sediments (Carapacha Formation). The extent of the Curacó basin is investigated using aeromagnetic data; its depocentre is conspicuously delineated by a narrow NNW-orientated magnetic low. In addition, scarce outcrops assigned to the same sequence are found on the Pampian continental crust, about 50 km to the east, in the proximity of the Valle Daza estate (Valle Daza sub-basin). The studied marine sequence of La Pampa is equivalent to other Lower to Middle Paleozoic units of the eastern margin of the Cuyania terrane and is clearly distinguished from the overlying Permian continental sedimentary sequence. U–Pb SHRIMP dating of detrital zircons from Valle Daza indicates a maximum deposition age of ca. 466 Ma; the minimum age is given by the intrusion of granites at ca. 405 Ma (i.e. Early Devonian). Geochemical data indicate that the Curacó basin was primarily sourced by an active continental margin, possibly the Ordovician Famatinian arc.

Keywords: Paleozoic marine foreland basin; Curacó basin; La Horqueta Formation; La Pampa province; U–Pb SHRIMP; Hf isotopes

1. Introduction

The basement of central La Pampa province, south-central Argentina (Fig. 1), comprises the southern portion of the Cuyania and Pampia terranes, amalgamated to the western margin of Gondwana during the Middle Ordovician and Cambrian times, respectively (Astini et al., 1996); their precise boundaries were defined by Chernicoff and Zappettini (2003, 2004a). The origin of the Cuyania terrane from Laurentia (e.g. Ramos, 2004; Vujovich et al., 2004a, Porcher et al., 2004, and references therein) or as a para-autochthonous part of Gondwana (e.g. Aceñolaza et al., 2002; Finney et al., 2003) remains a matter of debate in the geological community.

Adjacent to the Cuyania–Pampia terrane boundary, the depocentre of a Late Ordovician–Devonian foreland basin generated after the Middle Ordovician collision of Cuyania was recently identified (Chernicoff and Zappettini, 2003, 2004a,b, 2005a,b). This basin, herein referred to as the Curacó basin, was deposited on Cuyanian crust (Cuyania terrane) immediately to the west of the Pampia terrane. Its fill primarily comprises sandstones and shales of the La Horqueta Formation, which is

* Corresponding author. Council for Scientific and Technical Research (CONICET), Julio A. Roca 651, 1322 Buenos Aires, Argentina. Tel.: +54 11 4349 3148; fax: +54 11 4349 3171.
E-mail addresses: jchern@secind.mecon.gov.ar (C.J. Chernicoff), ezappe@secind.mecon.gov.ar (E.O. Zappettini), orestes.santos@bigpond.com (J.O.S. Santos), ebeyer@els.mq.edu.au (E. Beyer), nmcnaugh@cyllene.uwa.edu.au (N.J. McNaughton).

1342-937X/$ - see front matter © 2007 International Association for Gondwana Research. Published by Elsevier B.V. All rights reserved.
doi:10.1016/j.gr.2007.04.006

Please cite this article as: Chernicoff, C.J. et al. Foreland basin deposits associated with Cuyania accretion in La Pampa Province, Argentina. Gondwana Research (2007), doi:10.1016/j.gr.2007.04.006

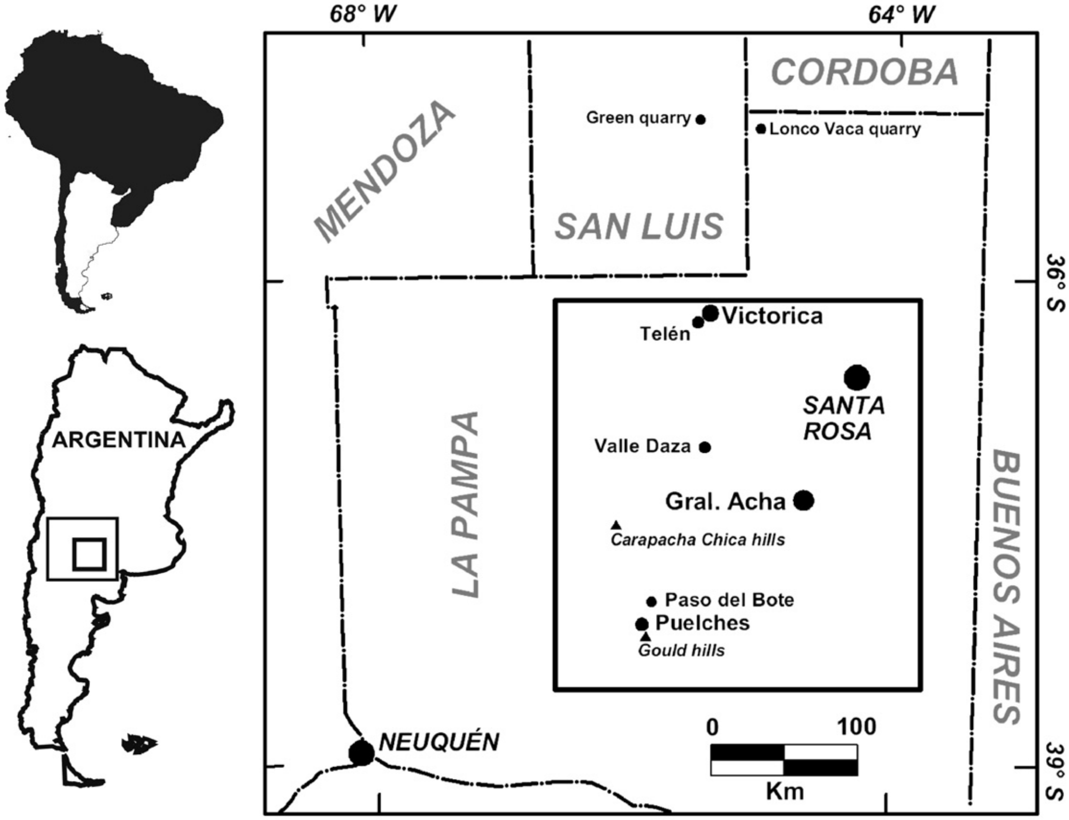

Fig. 1. Locality map of study region (rectangle in Curacó basin depocentre and greater study area, La Pampa province) and surrounding provinces of south-central Argentina. Sample MG40 collected at Valle Daza.

unconformably overlain by Permian continental sediments (Carapacha Formation). In addition, scarce outcrops assigned to the same sequence are found on the Pampian continental crust, about 50 km to the east, in the proximity of the Valle Daza estate (Valle Daza sub-basin). Drill-hole information also indicates the occurrence of buried Siluro-Devonian sandstones in the eastern part of La Pampa province (unpublished data of the Geological and Mining Survey of Argentina).

In the past, the bulk of the Paleozoic sediments of central La Pampa (i.e. Upper Ordovician–Devonian plus Permian) were undifferentiated and attributed to a single-age and single-origin unit, then regarded as a single formation. This was first defined as a Siluro-Devonian marine sequence named the Carapacha Formation (Vilela and Riggi, 1956), bearing Late Silurian brachiopods (Sgrosso, in Tapia, 1939). Criado Roqué (1972) correlated this unit with the La Horqueta Formation (exposed further north, in the San Rafael block of the Cuyania terrane); Linares et al. (1980) followed this assignment.

However, the discovery of a Permian flora of *Glossopteris* in a number of exposures in the Puelches area of La Pampa (Terraza, 1981; Terraza et al., 1982; Schultz, 1986; Melchor and Césari, 1991) led to the redefinition of the whole, undifferentiated Paleozoic sedimentary sequence as constituting a continental Lower Permian unit (Melchor, 1995, 1999). Fig. 2 shows the key outcrop sites of the La Horqueta Formation at the Curacó basin depocentre, near Puelches, also showing the key outcrop sites of the overlying Carapacha Formation.

2. Geological evidence

The major discrepancy concerning the age and setting of the Paleozoic sediments of central La Pampa referred to above has now been resolved as a result of new field observations, combined with geochronological, petrographical, geophysical and geochemical studies. The new data has indicated the presence of two unrelated sedimentary units separated by an unconformity. These units are:

1) A lower sequence, of Late Ordovician–Devonian age, composed of grayish green mudstones and sandstones (Fig. 3a), is herein referred to the La Horqueta Formation (in the sense of Baldis and Peralta, 1999). This unit was affected by low-grade regional metamorphism. The eastern outcrops at Valle Daza estate and surroundings show the effect of thermal metamorphism related to the intrusions of Devonian granitoids (e.g. Chacharramendi granite). Otherwise, the La Horqueta Formation is a unit mostly exposed further north, in the San Rafael Block of the Cuyania Terrane.
2) An upper sequence, composed of reddish gray conglomerates and sandstones (Fig. 3b), with minor limestones and pelites bearing a flora of *Glossopteris*. The term Carapacha Formation (Vilela and Riggi, 1956) is herein restricted to this upper sequence, of Permian age. Notably, the conglomerates of the upper sequence (Carapacha Formation) bear sandstone

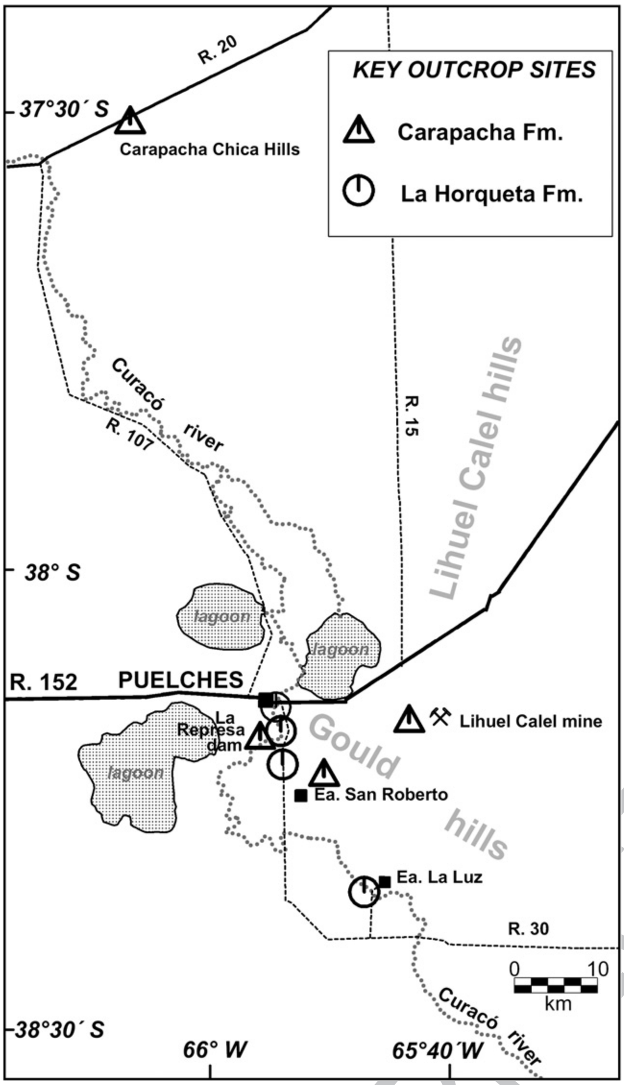

Fig. 2. Key outcrop sites of the La Horqueta Formation at the depocentre of the Curacó basin, La Pampa province (see location on Fig. 1). Main outcrop sites of overlying Carapacha Formation also shown.

clasts of the lower sequence (La Horqueta Formation); see Fig. 3c and d.

2.1. La Horqueta Formation

The La Horqueta Formation, within the Curacó basin depocentre, is exposed in the southern vicinity of the locality of Puelches as discontinuous outcrops on the bed of the Curacó river, from the proximity of the Puelches bridge, downstream up to at least the La Luz estate; smaller outcrops also are found in the Gould hills (Figs. 1 and 2).

From a petrographical point of view, this unit consists of a monotonous sequence of grayish green sandstones and pelites. The clastic fraction of the sandstone comprises grains of quartz and feldspar, and lithic grains, all of them being angular and ranging in size from 0.054 to 0.75 mm. The matrix reaches 10%, straddling the arenite/wacke boundary; it is partially recrystallized to an assemblage of epidote–chlorite and minor biotite–albite–titanite, indicating greenschist facies metamorphism. The alignment of biotite points to an incipient schistosity. The pelites contain very scarce angular lithic grains of volcanic rocks (partly replaced by calcite) and monomineralic grains of quartz, ranging 0.053–0.25 mm in size; they also, though rarely, contain grains of microcline, zircon and deformed muscovite. The matrix is argillaceous, largely recrystallized to illite.

SWIR reflectance spectrometry studies were applied to the sandstones, resulting in the identification of ammonium-illite, as well as chamosite and sheridanite, the latter two minerals being iron and magnesium chlorites, respectively. Ammonium-illite is indicative of the presence of organic matter (Williams and Ferrell, 1991). The occurrence of chamosite points to a shallow marine environment (e.g. Hallam and Bradshaw, 1979; Van Houten and Purucker, 1984; Schieber and Riciputi, 2004). Chamosite is known to be typical of marine deposits in Argentina of the same age range as the La Horqueta Formation, e.g. the Lipeón Formation (Boso and Monaldi, 1999), the Sierra Grande Formation (Zanettini, 1999), the Don Braulio Formation (Baldis and Peralta, 1999), as well as elsewhere in the world, e.g. the Clinton Formation (Cotter and Link, 1993) and the Red Mountain Formation (Chowns, 2002) in the USA, and the Djebilet Formation in Algeria (Guerrak, 1988). On the other hand, sheridanite is a good indicator of anoxic marine environment (Haïmeur, 1998); the local presence of authigenic pyrite in the sandstones is in agreement with this type of environment.

The eastern part of the Curacó basin sediments is poorly exposed in the Valle Daza estate and surroundings (Valle Daza sub-basin) (Fig. 1). In this area, the sequence also comprises sandstones affected by thermal metamorphism related to the intrusion of Devonian granitoids (evidenced by the formation of biotite–chlorite hornfels); locally, marked ductile deformation also affected this area. This sequence proved to be rich in detrital zircon and was sampled for U–Pb SHRIMP determinations (see below).

2.2. Carapacha Formation

The Carapacha Formation is exposed both in the Carapacha Chica hills and in the Puelches area (Figs. 1 and 2); in the latter area notable outcrops occur in the surroundings of the San Roberto estate (Gould hills), partially on the banks of the Curacó river (e.g. in the area known as the La Represa dam) and in the Lihuel Calel copper mine area.

The Carapacha Formation consists of sandstone (mostly quartzo-feldspathic), conglomerate, mudstone and limestone, which have been described previously in the Puelches area (e.g. Espejo and Silva Nieto, 1985; Melchor, 1995; Espejo and Silva Nieto, 1996). In the Carapacha Chica hills Melchor and Casadío (1999) report the occurrence of scarce limestone, in addition to fine- to medium-grained lithic sandstone and mudstone. SWIR reflectance spectrometry determinations applied to fine-grained sandstones revealed the presence of illite–smectite.

Particular attention was given to the conglomerates of this unit, since they consistently include sandstone clasts from the

Please cite this article as: Chernicoff, C.J. et al. Foreland basin deposits associated with Cuyania accretion in La Pampa Province, Argentina. Gondwana Research (2007), doi:10.1016/j.gr.2007.04.006

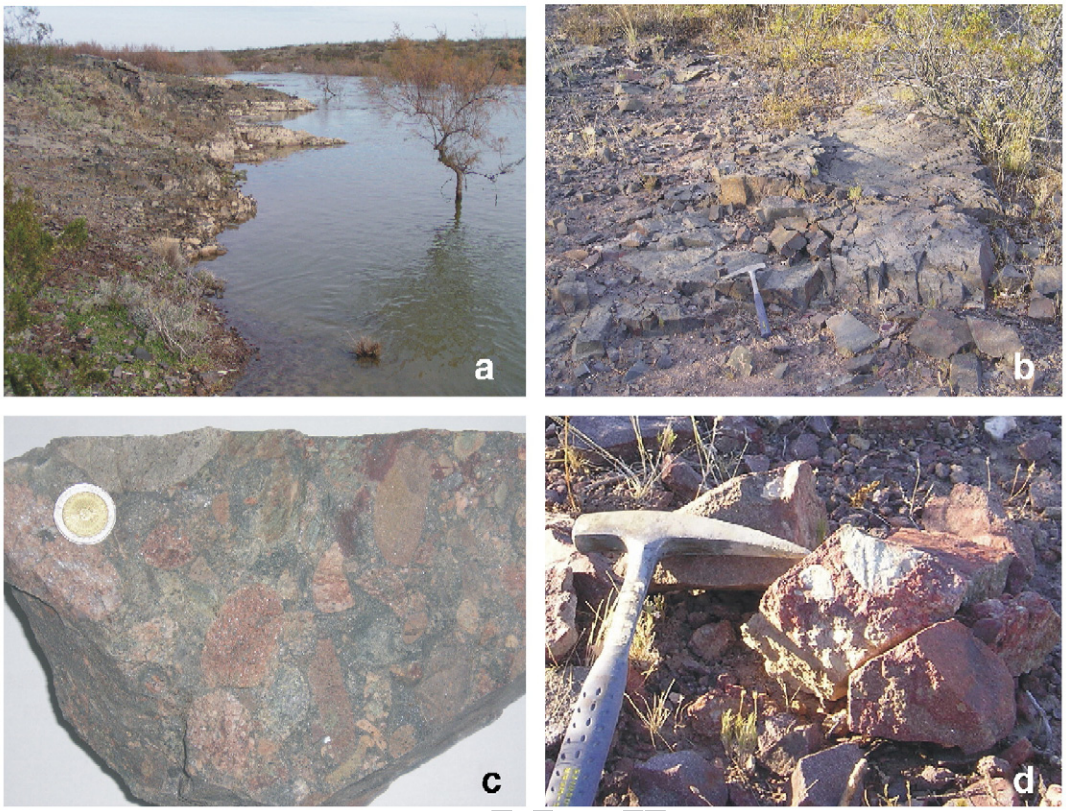

Fig. 3. a: Outcrops of sandstones of La Horqueta Formation (Puelches bridge).; b: Carapacha Formation sandstones (outcrop at La Represa dam); c: Carapacha Formation. conglomerates (Lihuel Calel copper mine area); d. Carapacha Formation. conglomerate (outcrop in the western Gould Hills).

lower sequence (La Horqueta Fm.), as shown on Fig. 3c and d. Sandstone clasts of the conglomerate are represented by angular monomineralic grains of quartz and feldspar, as well as angular lithic grains, ranging from 0.054 to 0.324 mm in size. It is notable that in the conglomerates of the western outcrops (i.e. San Roberto estate, La Represa dam; see Fig. 2) sandstone clasts are predominant, whereas the conglomerates of the eastern outcrops (i.e. Lihuel Calel copper mine area; see Fig. 2) are polymict, containing clasts of granitic, metamorphic and volcanic rocks. This lithological difference from west to east likely reflects the heterogeneous nature of the substrata.

3. Geophysical data

The aeromagnetic map of the study region is shown in Fig. 4a. The use of geophysical data in the study region has been critical in outlining important geological boundaries because of the scarcity of exposures; aeromagnetic data have the property of being able to see through the thin Quaternary cover.

The depocentre of the Curacó basin is depicted by a narrow NNW-oriented magnetic low that runs parallel and adjacent to the Cuyania–Pampia terrane boundary for at least 140 km. (Fig. 4a). The contribution of the thin overlying Permian sediments to this magnetic feature would be negligible. Fig. 4b (a geological interpretation or 'solid' geology map) shows the Curacó basin depocentre and the surrounding units (see also modeling of aeromagnetic data in Fig. 10).

4. Geochemical data

It is known that the geochemical signature of sediments is related to plate tectonic processes, i.e. different signatures reflect both different provenance and sedimentary processes (e.g. Bhatia and Crook, 1986). Consequently, a number of geochemical analyses were carried out on the La Horqueta Formation to contribute to the identification of its tectonic setting and provenance. The data reinforce the geological observations, i.e. the log (K_2O/Na_2O) vs. SiO_2 diagram of Roser and Korsch (1986) for sandstone–mudstone suites show that the sandstones of La Horqueta Formation plot in the *active continental margin* field (Fig. 5a). The provenance signatures of sandstone–mudstone suites were dealt with the discriminant function diagrams of Roser and Korsch (1988); the $f1/f2$ diagram (Fig. 5b) shows that sandstones have a *felsic igneous provenance*, coherent with an active continental margin.

In accordance with Bhatia and Crook's (1986) determination of tectonic settings of sedimentary basins, our results indicate that the La Horqueta Fm. sandstones were deposited in a sedimentary basin primarily sourced by an active continental margin.

In addition, chemical analysis was carried out on a 5 cm-wide rhyolitic clast from the conglomerates of the Permian Carapacha Formation in the Lihuel Calel copper mine area. Although it can only be considered as indicative, its major element content suggests a sub-alkaline volcanism (Fig. 5c)

Please cite this article as: Chernicoff, C.J. et al. Foreland basin deposits associated with Cuyania accretion in La Pampa Province, Argentina. Gondwana Research (2007), doi:10.1016/j.gr.2007.04.006

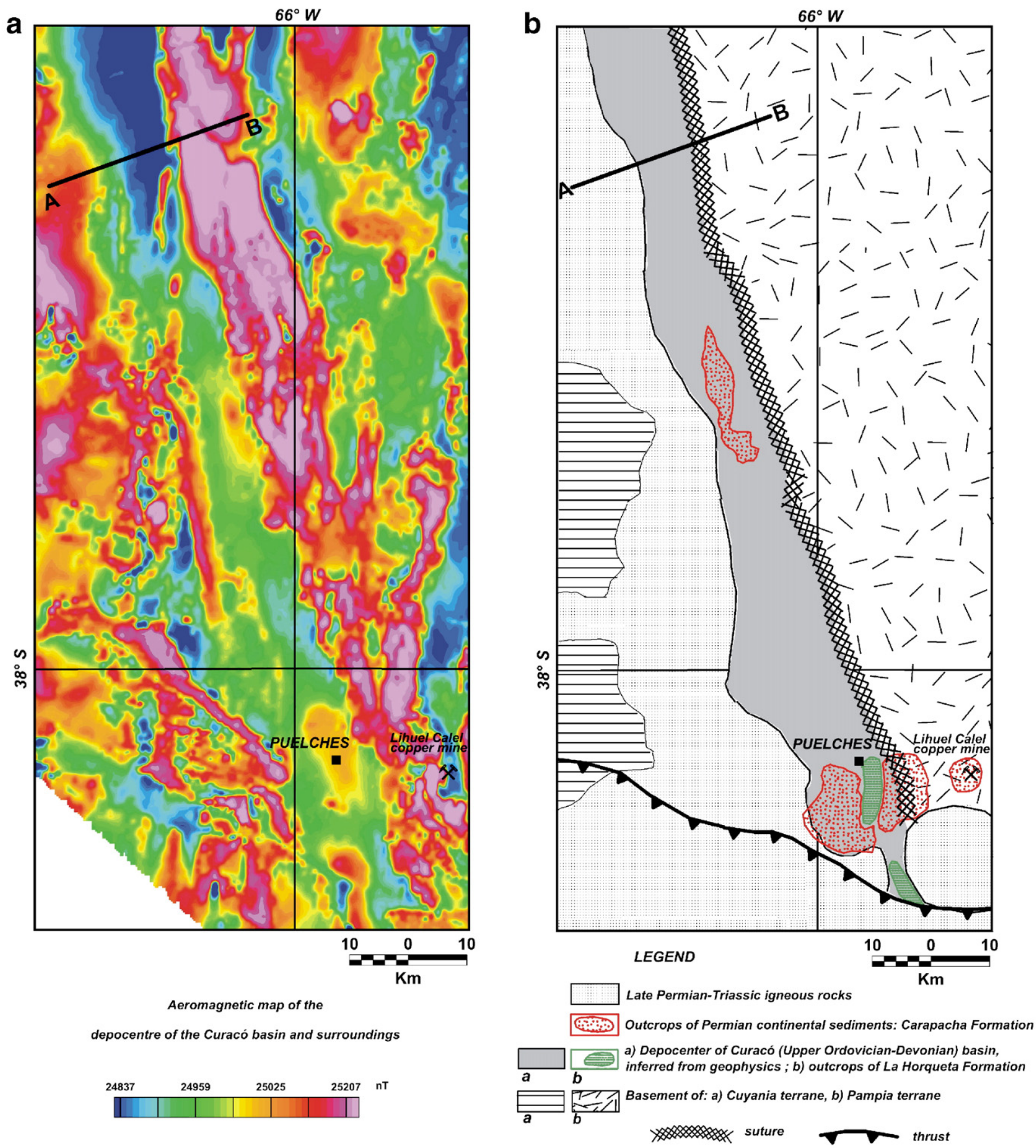

Fig. 4. (a) Aeromagnetic map of the Curacó basin depocentre and surroundings; (b) geological interpretation of the aeromagnetic data ('solid' geology map). AB: location of modelled transect (see Fig. 10a).

with peraluminous affinity (Fig. 5d). In the Rb–Y+Nb diagram of Pearce et al. (1984), the rhyolite plots in the volcanic arc field (Fig. 5e). The REE content of the La Horqueta sandstone was plotted normalized to NMORB (Fig. 5f). Since the principal factor that controls REE contents in clastic sediments is their provenance (e.g. McLennan, 1989), then the pattern shown on Fig. 5f could be considered to correspond to that of the source; the patterns of both the sandstone and the rhyolite point to an arc setting, compatible with the active margin field indicated in Fig. 5a. The nearby occurrence of meta-quartz diorites and meta-tonalites to the east of the Cuyania–Pampia boundary (e.g., at Paso del Bote, on the Pampia side of the terrane divide)

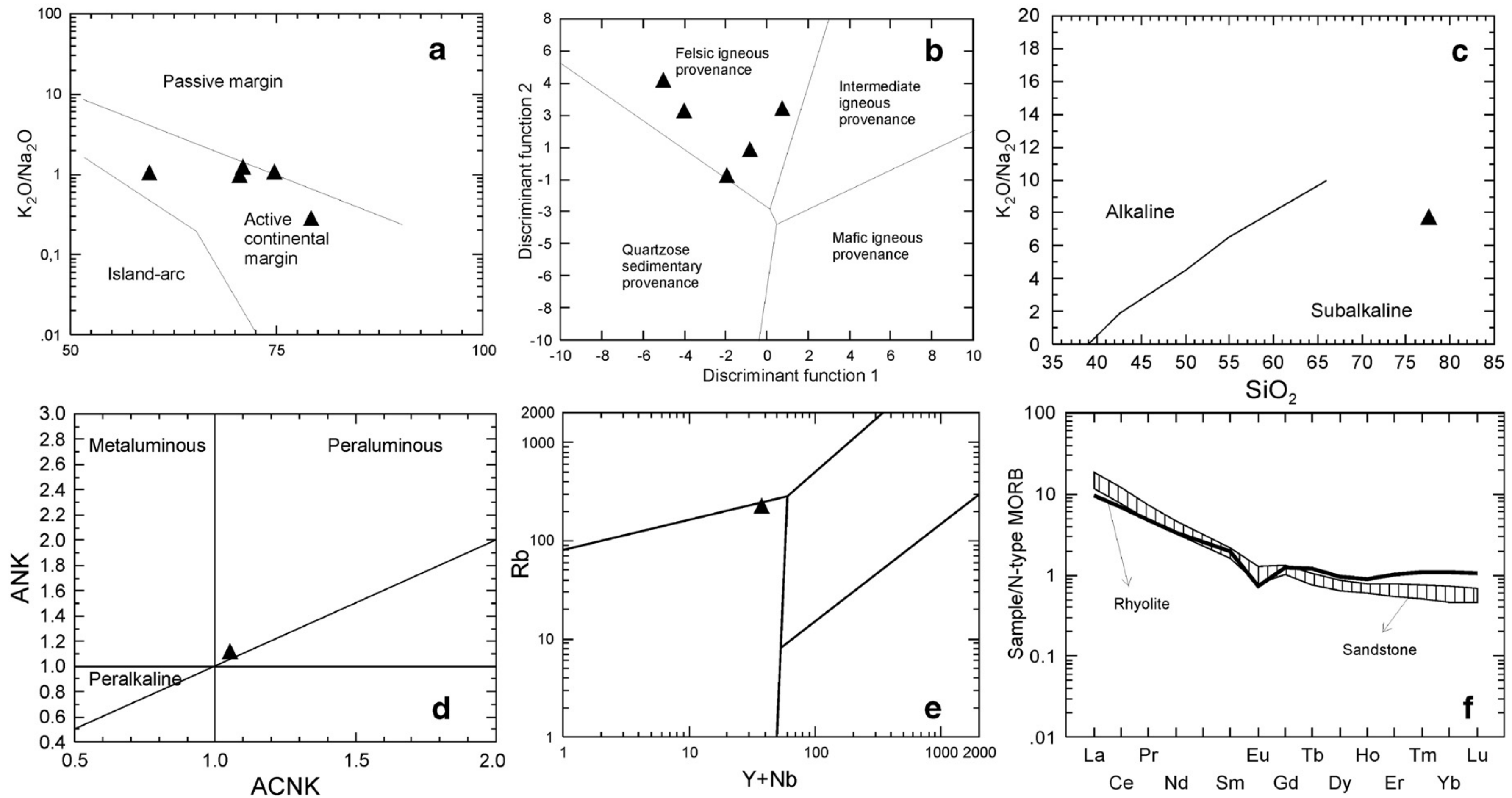

Fig. 5. Geochemical data for La Horqueta Formation sandstones plotted in (a) log (K_2O/Na_2O) vs. SiO_2 diagram of Roser and Korsch (1986); (b) the discriminant function diagram of Roser and Korsch (1988) showing: the discriminant functions employed are: $f1 = -1.773^*TiO_{2+}\ 0.607^*Al_2O_{3+}\ 0.76^*Fe_2O_{3-}\ 1.5^*MgO + 0.616^*CaO + 0.509^*Na_2O - 1.22^*K_2O - 9.09$ and $f2 = 0.445^*TiO_{2+}\ 0.07^*Al_2O_{3-}\ 0.25^*Fe_2O_{3-}\ 1.142^*MgO + 0.438^*CaO + 1.475^*Na_2O + 1.426^*K_2O - 6.861$; (c): total alkalis vs. SiO_2 diagram (rhyolite); (d) ANK–ACNK diagram (rhyolite); (e): Rb− (Y+Nb) discrimination diagram for acid rocks, applied to a rhyolitic clast from a Carapacha Formation conglomerate. The rhyolite falls in the VAG (volcanic arc) field; f: Rare-earth element abundances of sandstones and rhyolites normalized to NMORB.

Table 1
U–Pb SHRIMP and Hf isotopic data from detrital zircons of the La Horqueta Formation (sample MG40)

spot	U ppm	Th ppm	Th/U	4f206 (%)	Disc. %	Isotopic ratios $^{207}Pb/^{206}Pb$	$^{206}Pb/^{238}U$	$^{207}Pb/^{235}U$	$^{208}Pb/^{232}Th$	Ages $^{207}Pb/^{206}Pb$	$^{206}Pb/^{238}U$	T_{DMC} Hf	εHf
b.1-1	671	361	0.56	0.07	−0.5	0.05902±1.19	0.0925±1.09	0.7529±1.61	0.0283±1.59	568±26	570±6	1881	−6.96
b.1-2	874	771	0.91	0.21	−14.2	0.05639±1.46	0.0864±1.07	0.6718±1.81	0.0271±2.17	468±32	534±5	1550	−1.87
b.1-3	182	86	0.49	0.35	−30.0	0.05650±3.15	0.0999±1.39	0.7779±3.45	0.0306±3.43	472±70	614±8	1581	−1.34
b.2-1	184	3	0.02	−0.58	27.4	0.06085±4.58	0.0740±1.63	0.6206±4.86	−±−	634±99	460±7	1733	−5.90
b.2-2	377	175	0.48	0.55	35.3	0.09413±1.39	0.1637±1.14	21,252±1.80	0.0746±1.97	1511±26	978±10	2544	−12.80
b.2-3	173	3	0.02	1.43	1.4	0.04668±6.95	0.0690±1.29	0.5282±2.21	−±−	432±40	431±5	1622	−4.48
b.2-4	166	3	0.02	0.42	6.9	0.05711±3.77	0.0696±1.02	0.5484±3.90	− ±−	464±61	434±4	–	–
b.2-5	338	161	0.49	0.03	−0.1	0.05762±2.40	0.0833±0.81	0.6621±2.53	0.0266±2.28	515±53	516±4	861	9.38
b.3-1	400	357	0.92	0.05	0.8	0.06375±1.34	0.1195±1.20	10,503±1.80	0.0377±1.58	733±28	728±8	2082	−8.28
b.3-2	90	79	0.90	1.06	−26.3	0.05759±2.79	0.1047±1.82	0.8296±8.58	0.0324±5.00	509±184	642±11	1849	−5.47
b.3-3	223	3	0.01	1.32	1.2	0.06198±1.53	0.1101±1.46	0.9408±2.12	−±−	674±32	673±9	1950	−6.87
b.3-4	857	83	0.10	0.41	−23.2	0.05479±2.12	0.0802±1.12	0.6062±2.40	0.0190±11.86	404±47	498±5	1511	−1.68
b.3-5	455	279	0.63	0.19	−5.5	0.05728±1.72	0.0857±1.15	0.6768±2.06	0.0267±1.85	502±38	530±6	1448	−0.21
b.4-1	230	114	0.51	0.29	2.9	0.05808±3.95	0.0836±1.32	0.6693±4.16	0.0251±4.12	533±86	517±7	1503	−1.28
b.4-2	229	98	0.44	0.66	−35.4	0.05452±4.86	0.0860±1.33	0.6463±5.04	0.0252±5.44	393±109	532±7	1440	−0.05
b.6-1	209	274	1.35	0.32	2.4	0.05855±4.29	0.0869±1.29	0.7019±4.48	0.0269±2.26	551±94	537±7	1501	−1.00
b.6-2	83	86	1.07	0.00	9.9	0.05979±3.84	0.0868±2.03	0.7160±4.35	0.0268±3.18	596±83	537±10	1369	1.20
b.8-1	250	11	0.05	0.33	6.3	0.05695±2.54	0.0743±1.27	0.5832±2.84	−±−	490±55	461±6	1576	−3.25
b.8-2	573	6	0.01	0.24	−3.6	0.05595±1.43	0.0753±0.98	0.5808±1.74	−±−	450±31	468±4	1509	−2.05
b.9-1	50	38	0.80	0.27	5.0	0.05727±5.37	0.0875±2.64	0.7128±18.96	0.0276±12.02	569±120	541±14	1538	−1.58
b.10-1	174	77	0.45	0.51	14.8	0.06024±3.31	0.0843±1.16	0.6999±3.51	0.0239±3.55	612±72	522±6	1640	−3.53
b.10-2	595	245	0.43	0.07	1.3	0.05756±1.69	0.0818±0.62	0.6488±1.80	0.0253±1.76	513±37	507±3	1363	0.91
b.10-3	333	217	0.67	0.36	3.3	0.05789±3.35	0.0821±0.86	0.6550±3.46	0.0249±3.05	526±73	508±4	–	–
b.11-1	363	309	0.88	0.02	3.3	0.05948±1.91	0.0916±1.25	0.7516±2.28	0.0277±1.80	585±41	565±7	1563	−1.67
b.11-2	643	36	0.06	0.00	−14.8	0.05489±1.58	0.0753±0.64	0.5700±1.71	−±−	408±35	468±3	1649	−4.39
b.12-1	226	120	0.55	0.00	−1.0	0.05802±2.38	0.0867±1.00	0.6935±2.58	0.0271±2.21	530±52	536±5	1621	−3.02
b.13-1	253	127	0.52	0.17	5.2	0.05889±4.49	0.0865±1.28	0.7027±4.59	0.0265±4.38	564±96	535±7	1484	−0.75
b.14-1	105	97	0.95	0.10	19.3	0.06137±2.63	0.0851±1.62	0.7201±3.09	0.0267±2.59	652±56	526±8	1584	−2.53
b.15-1	210	99	0.49	0.13	7.3	0.05908±2.84	0.0854±1.33	0.6958±3.14	0.0262±3.24	570±62	528±7	1525	−1.51
b.15-2	1332	695	0.54	0.09	2.4	0.05854±0.98	0.0869±1.03	0.7016±1.42	0.0268±1.40	550±21	537±5	1431	0.18
b.15-3	194	80	0.42	0.33	−3.0	0.05902±3.76	0.0950±1.36	0.7729±4.00	0.0291±4.57	568±82	585±8	1806	−5.49
b.15-4	180	68	0.39	0.29	−39.2	0.06765±2.38	0.2034±1.49	18,972±2.81	0.0527±4.15	858±49	1194±16	1578	6.23
b.16-1	583	201	0.36	0.29	−12.8	0.05636±1.76	0.0851±1.11	0.6615±2.08	0.0260±2.53	467±39	527±6	1740	−5.16
b.16-2	229	3	0.01	0.55	−11.6	0.05155±4.49	0.0709±1.36	0.5325±2.51	−±−	389±47	442±6	1724	−6.01
b162b	204	3	0.01	0.29	−9.9	0.05318±2.84	0.0679±1.23	0.5074±2.03	−±−	381±36	423±5	1724	−6.01
b.16-4	214	3	0.01	0.69	−0.6	0.05859±2.47	0.0646±1.01	0.4876±6.22	−±−	401±138	405±4	–	–

Notes: Isotopic ratios errors in %. All Pb in ratios are radiogenic component corrected for ^{204}Pb (magmatic grains) and for ^{208}Pb (metamorphic grains).
disc. = discordance, as 100− 100{t[$^{206}Pb/^{238}U$]/t[$^{207}Pb/^{206}Pb$]}.
*f*206=(common ^{206}Pb)/(total measured ^{206}Pb) based on measured ^{204}Pb. Uncertainties are 1σ.
Hf model ages (T_{DMC}) calculated by projecting from the point back to the DM line with the slope of $^{176}Lu/^{177}Hf$ of the average continental crust (0.015).
εHf values calculated at the $^{206}Pb/^{238}U$ age of each grain (*T*). For grain b.2-2 (1511 Ma) the εHf is calculated at the $^{207}Pb/^{206}Pb$ age.

is interpreted as forming part of the Famatinian magmatic arc at these latitudes (Villar et al., 2005), being one of the sources for the foreland sequence.

5. Geochronological data

5.1. Methodology

The combination of U/Pb SHRIMP and Hf isotopic determinations for individual zircon grains provides not only the age but the nature and source of the host magma, whether crustal or juvenile mantle, and model age (TDM) of the provenance. This integrated analysis, applied to suites of detrital zircon, gives a more distinctive, and more easily interpreted, picture of crustal evolution in the provenance area than age data alone (Veevers et al., 2006 and references therein).

Sample MG40 (La Horqueta Formation sandstone, collected at Valle Daza, see Fig. 1) was crushed, milled, sieved, and washed to remove very fine material (clay and silt sizes). The 60–250 mesh fraction was treated with heavy liquids (to remove light minerals) and magnetic separator (to concentrate the less magnetic minerals such as zircon). Zircon was hand-picked and organized in an epoxy mount, which was polished and carbon-coated for SEM (Scanning Electron Microscope) study. Back-scattered images (BSE) were taken using a JEOL6400 SEM at the Centre for Microscopy and Microanalyses at University of Western Australia. Images of zircon are critical for identifying internal features such as core and rims and to help avoiding areas with high common lead content (inclusions, fractures, and metamict areas). Epoxy mount (UWA 05-85) was gold-coated for SHRIMP analyses. The SHRIMP analytical spot was about 25 μm in diameter and four or five

Table 2
Hf isotopic data of detrital zircons of La Horqueta Formation (sample MG40)

Spot	$^{176}Hf/^{177}Hf$	Error (1σ)	$^{176}Lu/^{177}Hf$	$^{176}Yb/^{177}Hf$	$^{176}Hf/^{177}Hf$ [a]	ε Hf [b]	Error (1σ)	T (DM) [c]	T (DMC) [c]
b.1-1	0.28222	0.000023	0.00194666	0.053958	0.282198	−6.96	0.81	1405	1881
b.1-2	0.282381	0.000016	0.00143786	0.0391458	0.282366	−1.87	0.56	1172	1550
b.1-3	0.282343	0.000017	0.00124685	0.0338109	0.282328	−1.34	0.60	1216	1581
b.2-1	0.28232	0.000014	0.00207471	0.0629541	0.282301	−5.90	0.49	1275	1733
b.2-2	0.281785	0.000016	0.00122583	0.0347323	0.281761	−12.80	0.56	1949	2544
b.2-3	0.282377	0.000014	0.00157796	0.0573852	0.282364	−4.48	0.49	1182	1622
b.2-5	0.282712	0.000088	0.00162351	0.0582891	0.282695	9.38	3.08	732	861
b.3-1	0.282081	0.000011	0.00173381	0.0531554	0.282056	−8.28	0.39	1583	2082
b.3-2	0.282203	0.000012	0.000846887	0.0300035	0.282192	−5.47	0.42	1387	1849
b.3-3	0.282148	0.0000088	0.000828239	0.0373397	0.282137	−6.87	0.31	1458	1950
b.3-4	0.282407	0.000015	0.0011885	0.0473298	0.282395	−1.68	0.53	1130	1511
b.3-5	0.282439	0.000024	0.00223985	0.0645022	0.282415	−0.21	0.84	1119	1448
b.4-1	0.282403	0.000016	0.000940008	0.0293613	0.282393	−1.28	0.56	1128	1503
b.4-2	0.282435	0.000015	0.00153125	0.0541977	0.282419	−0.05	0.53	1103	1440
b.6-1	0.282407	0.0000093	0.00177882	0.0648706	0.282388	−1.00	0.33	1148	1501
b.6-2	0.282464	0.0000083	0.00125751	0.0469492	0.282451	1.20	0.29	1056	1369
b.8−1	0.28239	0.000011	0.00162564	0.0596392	0.282375	−3.25	0.39	1166	1576
b.8-2	0.282423	0.000014	0.00191988	0.0736707	0.282405	−2.05	0.49	1130	1509
b.9-1	0.28238	0.000011	0.000975949	0.0345144	0.282369	−1.58	0.39	1159	1538
b.10-1	0.282338	0.000011	0.00103629	0.0377526	0.282327	−3.53	0.39	1216	1640
b.10-2	0.282476	0.000015	0.00134047	0.0538636	0.282462	0.91	0.53	1042	1363
b.11-1	0.282368	0.000017	0.0015364	0.0446466	0.282351	−1.67	0.60	1192	1563
b.11-2	0.282346	0.000014	0.000821627	0.0310171	0.282338	−4.39	0.49	1199	1649
b.12-1	0.28234	0.000013	0.00075409	0.0279602	0.282332	−3.02	0.46	1204	1621
b.13-1	0.282416	0.000011	0.00179856	0.0666414	0.282397	−0.75	0.39	1136	1484
b.14-1	0.282374	0.00002	0.00207405	0.0642165	0.282352	−2.53	0.70	1202	1584
b.15-1	0.282398	0.000012	0.00173746	0.0458819	0.282380	−1.51	0.42	1159	1525
b.15-2	0.28244	0.0000075	0.00173222	0.0641331	0.282421	0.18	0.26	1102	1431
b.15-3	0.28224	0.00001	0.000891006	0.0278622	0.282230	−5.49	0.35	1340	1806
b.15-4	0.282171	0.0000074	0.000774865	0.0251225	0.282152	6.23	0.26	1426	1578
b.16-1	0.282295	0.000021	0.00163246	0.0470949	0.282278	−5.16	0.74	1293	1740
b.16-2	0.282329	0.000011	0.00205386	0.0579325	0.282311	−6.01	0.39	1262	1724

Assumed $^{176}Lu/^{177}Hf$ and $^{176}Hf/^{177}Hf$ values are respectively 0.0332 and 0.282772 for CHUR, and 0.0384 and 0.283251 for DM.
TDM is calculated by projecting from the point back to the DM line using the zircon $^{176}Lu/^{177}Hf$ ratio.
T_{DMC} (crustal) is calculated by projecting from the point back to the DM line with the slope of $^{176}Lu/^{177}Hf$ of the average continental crust (0.015).
[a] Initial ratio, ^{176}Lu decay constant = 1.983 × 10−11 (Bizzarro et al., 2003).
[b] ε calculated according to the U–Pb ages of Table 1.
[c] Model ages in Ma.

scans were used for each spot-analysis. Both $^{206}Pb/^{238}U$ and $^{207}Pb/^{206}Pb$ ages are presented in Table 1 but $^{206}Pb/^{238}U$ ages are used for the ages in cumulative plots and for individual grains except for Mesoproterozoic grain b.2–2. The uncertainties of individual ages are quoted at 1σ whereas the final ages and those used in the plots are calculated at 2σ level (about 95% confidence). SHRIMP data were reduced using SQUID software (Ludwig, 2001) and plots are prepared using ISOPLOT/Ex (Ludwig, 2003).

Hf-isotope analyses reported here were carried out in situ using a New Wave Research LUV213 laser-ablation microprobe, attached to a Nu Plasma multicollector ICPMS at GEMOC Key Centre, Macquarie University, Sydney. Most analyses are carried out with a beam diameter of about 40 µm, a 10 Hz repetition rate, and energies of 0.6–1.3 mJ/pulse. Typical ablation times are 30–120 s, resulting in pits 20–40 µm deep. The analytical spots of Hf-isotope analyses were located in the same site of the previous U–Pb SHRIMP analyses.

Isobaric interferences of ^{176}Lu and ^{176}Yb on ^{176}Hf were corrected by the Nu Plasma because the mass bias of the instrument is independent of mass over the mass range considered. Interference of ^{176}Lu on ^{176}Hf is corrected by measuring the intensity of the interference-free ^{175}Lu isotope and using $^{176}Lu/^{175}Lu=0.02669$ to calculate the intensity of ^{176}Lu. Similarly, the interference of ^{176}Yb on ^{176}Hf is corrected by measuring the interference-free ^{172}Yb isotope and using $^{176}Yb/^{172}Yb$ to calculate the intensity of ^{176}Yb. The spiking of JMC475 Hf standard is used to determine the value of $^{176}Yb/^{172}Yb$ (0.5865) required to yield the value of $^{176}Hf/^{177}Hf$ obtained on the pure Hf solution.

The ^{176}Lu decay constant used to calculate initial $^{176}Hf/^{177}Hf$, εHf values, and model age is 1.983×10^{-11} (Bizzarro et al., 2003). Typical uncertainties on single $^{176}Lu/^{177}Hf$ analyses are about 1 epsilon unit (±0.001–0.002%) incorporating both spatial variation of Lu/Hf and analytical uncertainties. Hf data are given in Table 2. εHf values, also summarized in Table 1, were calculated at the $^{206}Pb/^{238}U$ age of each grain (T).

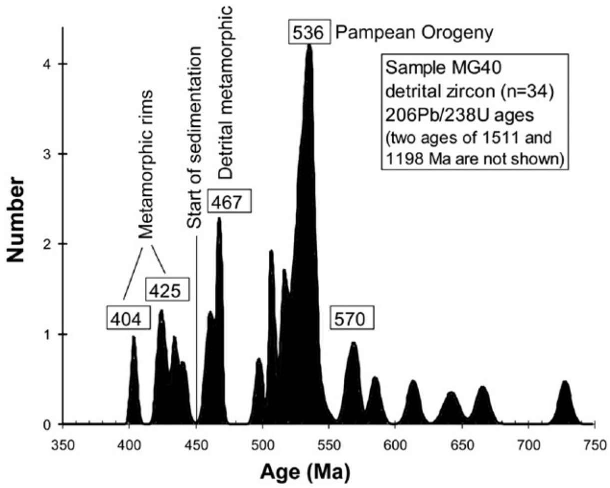

Fig. 6. Cumulative probability plot of ^{206}Pb–^{238}U isotopic ages of detrital zircons (n=36) from the La Horqueta Formation, sampled at Valle Daza. Two Mesoproterozoic ages are not shown. Youngest metamorphic grain: 405±4 Ma.

For grain b.2–2 the εHf is calculated at the $^{207}Pb/^{206}Pb$ age (1511 Ma).

5.2. Results and evaluation

5.2.1. Zircon U–Pb SHRIMP dating

36 detrital zircons were analysed with the SHRIMP to detect the major sources for the basin deposition. Most of grains are Cambrian (n=17) or Neoproterozoic (n=8) in age, followed by Ordovician (n=4), and scarce Silurian–Early Devonian (n=5). There are two highly discordant Mesoproterozoic grains. 35 out of 36 grains are interpreted as magmatic, with 10 displaying metamorphic rims (n=7) or zones (n=2). The metamorphic areas are identified by two main features: the lack of zoning and the very low Th/U ratios (Vavra et al., 1999). One grain (3.3) has a metamorphic core (673 Ma) surrounded by an igneous rim. The metamorphic

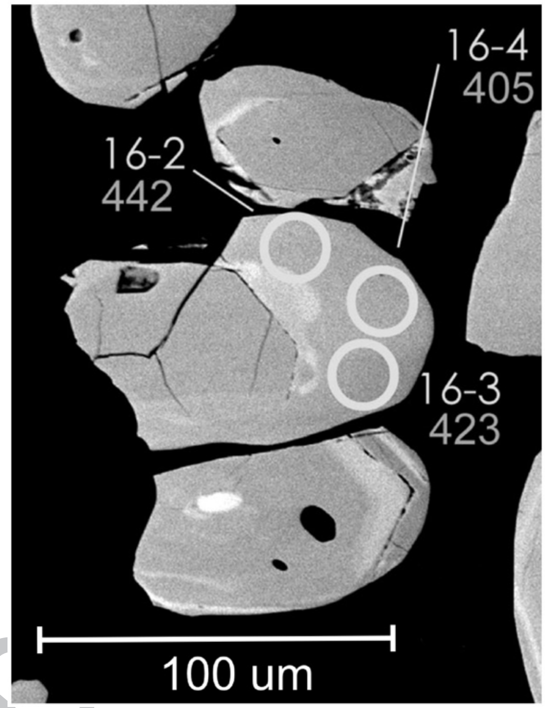

Fig. 8. Back-scattered image of zircon b.16–2. The three SHRIMP spots are located in the same rim and displaying different ages (442, 423, and 405 Ma), which suggests isotopic disturbance.

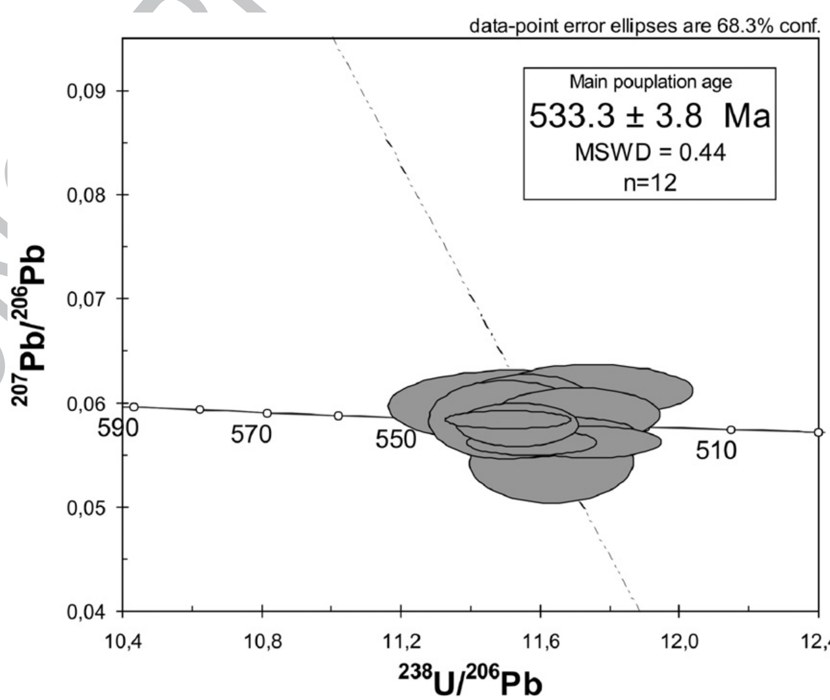

Fig. 7. Inverse concordia plot ($^{207}Pb/^{206}Pb$ vs. $^{206}Pb/^{238}U$) of Cambrian detrital magmatic zircons providing an age of 533.3±3.8 Ma (MSWD=0.44).

Please cite this article as: Chernicoff, C.J. et al. Foreland basin deposits associated with Cuyania accretion in La Pampa Province, Argentina. Gondwana Research (2007), doi:10.1016/j.gr.2007.04.006

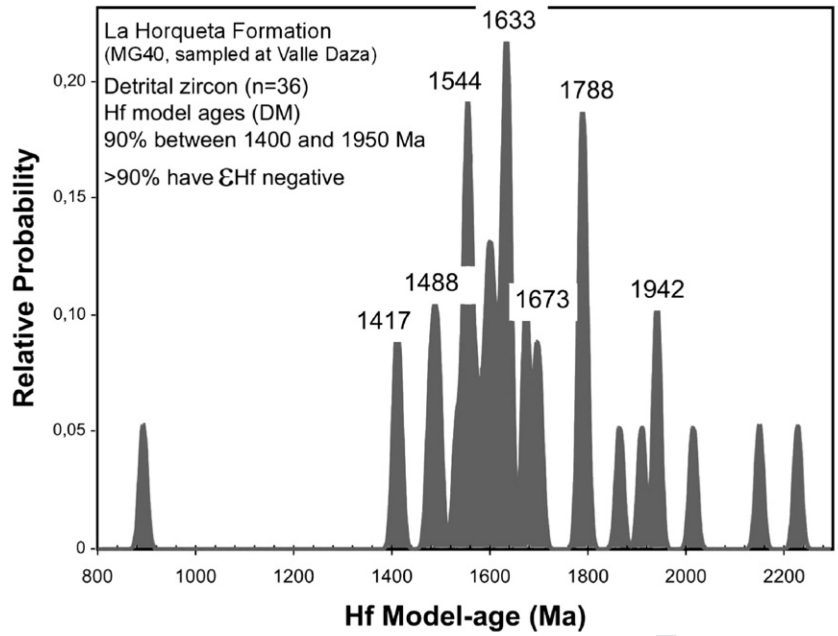

Fig. 9. Cumulative probability plot (Ludwig, 2003) of 36 Hf model ages (depleted mantle model).

zones have Th/U ratios between 0.01 and 0.06, much lower than the magmatic areas (0.10–1.58). The proportion of zircons having metamorphic areas (about 28%) is relatively high considering other examples of detrital studies in South America cratons (Hartmann and Santos, 2004). This may reflect the abundance of metamorphic rocks in the source area and/or an immature nature of the foreland sequence. The cumulative probability plot (Fig. 6) shows four main populations of ages at 425 Ma ($n=3$), 467 Ma ($n=4$), 536 Ma ($n=13$), and 570 Ma ($n=2$). The two main Paleozoic populations correspond respectively to a lower concordia intercept age of 533.3±3.8 Ma ($n=12$, Fig. 7) and weighted mean age of 465.9±2.3 Ma ($n=4$). Thus the major sources of the Valle Daza sub-basin are dominantly represented by Neoproterozoic–Cambrian magmatic zircons derived from the Pampean arc (recycled or not in the sedimentary sequence metamorphosed at ca. 466 Ma and exposed at Paso del Bote — see below).

All the analysed Ordovician zircons and zircon rims are metamorphic, which suggests an important contribution to the foreland sequence from exhumed metamorphic rocks (~466 Ma). There are five metamorphic rims with ages scattered between 442 Ma (earliest Silurian) and 405 Ma (Early Devonian). Metamorphic grains tend to survive less well during transport and recycling when compared to magmatic grains, because on average they are richer in U (Hartmann and Santos, 2004). The presence of these metamorphic zircons (dominantly of Ordovician–Early Silurian age) indicates that the metamorphic orogenic core was exposed, forming a major contribution to the foreland fill. Transportation of grains was possibly short.

The weighted mean $^{206}Pb/^{238}U$ age of the main population of detrital metamorphic zircons of 466±2 Ma (Middle Ordovician) corresponds to the maximum age for the onset of sedimentation, indicating that deposition probably started during the Late Ordovician. This age of metamorphism corresponds to the collisional event of Cuyania and Pampia terranes (Astini et al., 1996), and is comparable to a U–Pb age determined in fully recrystallized zircons obtained by the present authors in biotite–garnet paraschists at Paso del Bote (unpublished data). Previous Middle Ordovician U–Pb ages have been obtained for metamorphic zircon from several outcrops in the Sierras Pampeanas (Baldo et al., 2001; Casquet et al., 2001; Rapela et al., 2001; Vujovich et al., 2004b). The 405–442 Ma range obtained is interpreted as a resetting of rims of zircons because of the thermal metamorphism that affected the sequence related to the intrusion of Devonian granitoids at 405 Ma. Irregular metamorphic re-setting of U–Pb ages is suggested by the presence of three different ages (442 Ma, 423 Ma and 405 Ma) in the same rim of a single grain (Fig. 8).

5.2.2. Hf isotopes

The Hf isotope composition of dated zircons provides a characteristic signature of the protolith and information as to

Fig. 10. Geotectonic model. a: schematic model of the aeromagnetic data; b: geological correspondence of schematic model; c: regional framework (not to scale); d: Curacó basin in the context of the map of accreted terranes in the southern region of South America (modified from Chernicoff and Zappettini, 2004a,b); e: closer view of the terrane map of central Argentina, with indication of exposures of Ordovician–Devonian marine foreland sediments related with Cuyania accretion (1: Precordillera, 2: San Rafael Block; 3: Puelches, 4: Valle Daza). Reference: Relative magnetic susceptibilities used for modelling: Cuyania and Pampia terranes 0.02 SI, slivers of high-susceptibility material (mostly Famatinian magmatic arc) in the Pampia terrane 0.0368 to 0.0883 SI, depocentre of Curacó basin (mostly La Horqueta Formation, magnetically undifferentiated from the Carapacha Formation) −0.003 SI.

Please cite this article as: Chernicoff, C.J. et al. Foreland basin deposits associated with Cuyania accretion in La Pampa Province, Argentina. Gondwana Research (2007), doi:10.1016/j.gr.2007.04.006

crustal residence time. The former is expressed as $\varepsilon Hf(T)$ values, which compare the $^{177}Hf/^{176}Hf$ ratios at the time of crystallization to a Chondritic Uniform Reservoir (CHUR).

The analysed Ordovician zircons show $^{176}Hf/^{177}Hf$ ratios corresponding to $\varepsilon Hf(T)$ from −2.05 to −4.39. The $\varepsilon Hf(T)$ values of the Cambrian zircons range from −5.16 to +1.20

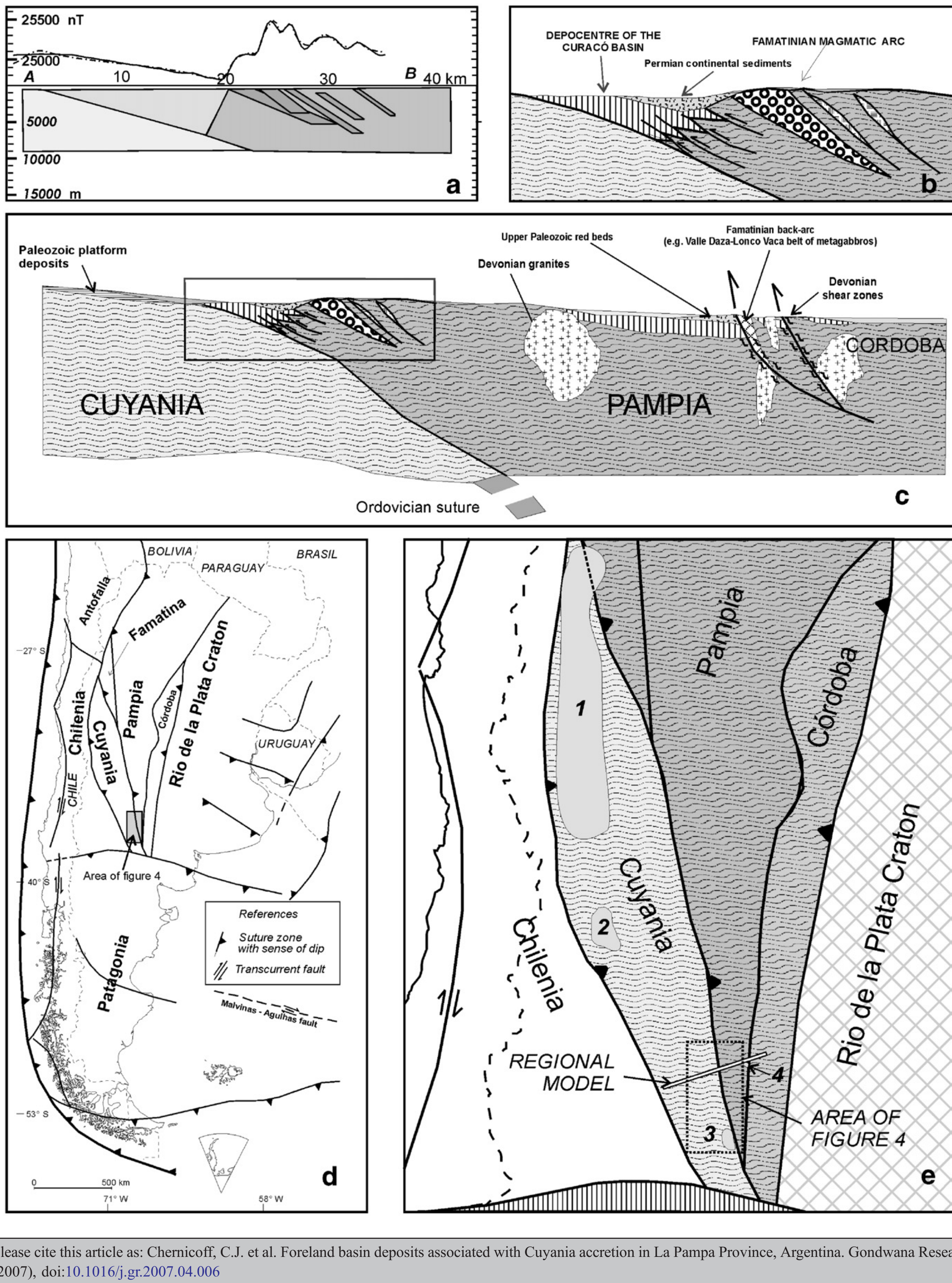

and those of the Neoproterozoic zircons from −8.28 to −1.34. The discordant Mesoproterozoic zircons have anomalous εHf(T) values. The predominance of detrital zircons with negative εHf(T) (>90%) strongly suggests that their primary sources contained large amounts of older recycled crustal components. Only b.2–5 shows evidence of a more juvenile source.

Hf TDM model ages give an estimated age for the source material of the magma from which the zircon crystallized, a concept comparable to Nd model ages. TDM model ages calculated using the measured $^{176}Lu/^{177}Hf$ of the zircon can only give a minimum age of the source material. Therefore, a 'crustal' model age T_{DMC} has also been calculated for each zircon, which assumes that its parental magma was produced from an average continental crust ($^{176}Lu/^{177}Hf=0.015$) that originally was derived from the depleted mantle. T_{DMC} gives optimum ages. The Hf T_{DMC} model ages for MG40 are shown in a cumulative probability plot in Fig. 9. They range between 900 and 2100 Ma, but 90% of the data is concentrated in the 1400–1950 Ma time interval. There are seven main peaks, at 1417 Ma, 1488 Ma, 1544 Ma, 1633 Ma, 1673 Ma, 1788 Ma, and 1942 Ma. The Hf isotopic data, together with the U–Pb ages, suggest that the Neoproterozoic–Cambrian zircons were derived from a reworked crust with Hf T_{DMC} model ages between 1.4 and 1.95 Ga; the TDM ages suggest that the minimum age of the source material is 1.0–1.4 Ga.

Although there are no Hf TDM model ages for the Pampia terrane and the Río de la Plata Craton, the Sm–Nd TDM model ages available for the Pampia–Córdoba terrane fall mainly within the 1.5–1.8 Ga age range (Rapela et al., 1998; Leal et al., 2003) and therefore coincide with the Hf TDM model ages presented here. In contrast, most crustal residence ages of the Rio de la Plata craton are higher than 2 Ga (Hartmann et al., 2002; Hartmann et al., 2003; Leal et al., 2003; Rapela et al., 2005), which precludes the latter craton as an indirect source for the analyzed zircons.

Our interpretation of the Hf isotopic data is that the crustal rocks of 1.4–1.95 Ga would form part of the present-day substratum (no exposures reported) of the Pampia–Córdoba terrane, and that they would not have been exhumed during the depositional time of the Curacó basin (Late Ordovician–Devonian) due to the absence of detrital zircons of that age. The observed range of Proterozoic Hf T_{DMC} model ages of the dated zircons suggests that this substratum would correspond to an orogen of 1.4–1.95 Ga, partially coeval with the Juruena orogen (Santos, 2003) accreted to the nucleus of the Amazon craton in northern and central Brazil.

6. The proposed geotectonic model

The proposed model is a foreland basin filled by Upper Ordovician–Devonian marine sediments of the La Horqueta Formation, unconformably covered by Permian continental deposits of the Carapacha Formation. The depocentre of the foreland basin developed on the Cuyania side of the Cuyania–Pampia boundary, with sediments also reaching the Pampia terrane to the east (e.g. Valle Daza sub-basin).

Fig. 10a depicts a schematic model based on geophysical data (an aeromagnetic transect over the Cuyania–Pampia boundary zone, also encompassing the Curacó basin depocentre), whereas Fig. 10b shows its geological correspondence. The main feature of the transect is the central magnetic low caused by the non-magnetic sediments of the La Horqueta Formation, and its pronounced asymmetry which reflects the shape of the depocentre, i.e. a steeply dipping eastern slope and a gentle dipping western slope. The flanking Cuyania and Pampia basements have similar, moderately magnetic signatures. In addition, the Pampia (or eastern) segment of the transect shows a number of magnetic highs of short wave-length arising from upthrust slivers of the Famatinian magmatic arc, mostly buried at these latitudes, though identified e.g. at Paso del Bote (Villar et al., 2005).

Fig. 10c shows the model in the scope of a more regional framework. This sketch extends farther east than the previous ones. It depicts the Valle Daza sub-basin, and the Early Devonian granitic intrusions and late Devonian shear zones that locally affect the sediments of the La Horqueta Formation. In addition, the Valle Daza-Lonco Vaca belt of metagabbros, thought to represent the Famatinian back-arc at these latitudes (Chernicoff and Zappettini, 2004a,b; Chernicoff et al., 2005; Zappettini et al., 2005; Chernicoff et al., in press), is also shown. One of the late Devonian shear zones (later reactivated during the Cenozoic) separates the belt of metagabbros from Upper Paleozoic red beds (Chernicoff and Zappettini, 2005c; Chernicoff and Zappettini, in press). Finally, Fig. 10d and e show the regional tectonic context of the Curacó basin in plan view. Fig. 10e, in particular, is meant to show the northern equivalents of the Curacó basin sediments in Cuyania, i.e. in the Precordillera (No. 1) and in the San Rafael block (No. 2).

The geometry of the Curacó basin depocentre is consistent with eastward-dipping subduction leading to the Cuyania–Pampia collision, and the associated synthetic thrusts. The proposed model also explains the provenance of sediments derived from the Famatinian orogen.

7. Summary and discussion

The present study led to the identification of two sedimentary sequences, formerly undifferentiated and attributed to a single-age and single-origin unit, the Carapacha Formation (firstly defined as marine Siluro-Devonian, and later redefined as continental Permian). This major discrepancy was largely due to the scarcity of exposures, since the province of La Pampa in south-central Argentina is mainly a region of very low relief and widely covered by Quaternary sediments.

New data, based on new field observations, as well as geochronological, petrographical, geophysical and geochemical studies, identified two unrelated sedimentary units separated by an unconformity: 1) a lower sequence of Late Ordovician–Devonian age, composed of grayish green pelite and sandstone herein referred to as the La Horqueta Formation (in the sense of Baldis and Peralta, 1999), and 2) an upper continental Permian-age sequence, composed of reddish gray conglomerate

Please cite this article as: Chernicoff, C.J. et al. Foreland basin deposits associated with Cuyania accretion in La Pampa Province, Argentina. Gondwana Research (2007), doi:10.1016/j.gr.2007.04.006

and sandstone, with minor limestone and pelite containing a *Glossopteris* flora, referred to herein as the Carapacha Formation.

The oldest sequence comprises marine sediments, representing the southern continuation of the same unit exposed in the San Rafael Block of the Cuyania terrane. These sediments were deposited on continental crust with a depocentre — conspicuously delineated by a narrow NNW-oriented magnetic low— developed on the Cuyania side of the Cuyania–Pampia boundary. In addition to this depocentre, these sediments were also deposited on the Pampia terrane to the east (e.g. Valle Daza sub-basin); the latter sediments display the effect of thermal metamorphism related to the intrusion of Early Devonian granitoids, which would set their minimum age at ca. 405 Ma.

The geotectonic setting of these marine sediments is interpreted as corresponding to a foreland basin, herein referred to as the Curacó basin, related to the accretion of Cuyania to Gondwana. The deformation (folding and thrusting) of the foreland basin sediments is considered to have occurred during the late Devonian (Chanic phase of the Famatinian orogeny), related to the docking of the Chilenia terrane.

The sequence is equivalent to other Lower to Middle Paleozoic units of the eastern margin of the Cuyania terrane, and it forms part of the *Foreland Basin I* of Ramos (2000; Table 1). The latter model differs from the scheme of Astini et al. (1996), for whom the deposits accumulated during the interval between the collision of Cuyania and the accretion of Chilenia belong to the *Foreland Basin II stage.*

The Upper Ordovician Pavón Formation (Caradoc biostratigraphic age ~455 Ma), exposed further north, in the San Rafael Block of Cuyania, was described by Cingolani et al. (2003) as a sequence deposited in a foreland basin generated after the accretion of Cuyania. The latter authors also indicate that the important vertical (rather than lateral) facies changes produced by the progradational system of the Pavón Formation suggest deposition in a linear trough; although its orientation was not established, this trough could well represent the northern extension of the narrow, NNW-orientated depocentre of the Curacó basin. This unit would correlate with the lower portion of the Curacó basin sediments.

Geochronological data indicate that the detrital zircons in the sequence show pre-depositional metamorphic growth dated at ca. 466 Ma, during the Famatinian docking of the Cuyania terrane with Pampia. The provenance of the ca. 536 Ma magmatic zircons can be related to the Pampean magmatic arc. Most of the zircons have negative εHf(T) (>90%) and Hf crustal model ages (T_{DMC}) of between 1400 and 1950 Ma, which strongly suggests that their Neoproterozoic–Cambrian sources contained large amounts of older crustal components. They are not, however, represented by older detrital zircons, indicating that the older crustal components were not exhumed during the sedimentation in the Curacó basin.

Though the origin of the Permian unit (Carapacha Formation) goes beyond the scope of this work, these rocks could have formed as foreland basin deposits related to the Late Paleozoic accretion of the Patagonia terrane (Ramos, 1984; Pankhurst et al., 2006). Permian foreland basin deposits occur in the Sierra de la Ventana fold belt (e.g. Lopez Gamundi et al., 1995), and the Carapacha Formation could possibly represent fragments of the (Permian) foreland deposits controlled by the roughly N–S trending relief of the basement prevalent during Permian times (Chernicoff and Zappettini, 2005c). The study of the origin of the Permian sediments known to exist in the subsurface of the La Pampa region (e.g. Dirección Nacional de Geología y Minería, 1958; Kostadinoff and Llambías, 2002) may help to corroborate the latter assertion.

8. Uncited reference

Bodet and Scharer, 2000

Acknowledgments

This work is supported by CONICET Research Grant PIP-5008 to Carlos J. Chernicoff. SEGEMAR provided aeromagnetic data and logistical support. We wish to thank Cees van Staal and James Gleason for their careful reviews of the manuscript. We also owe a debt of gratitude to Robert Pankhurst for his helpful comments, in addition to his thorough editing of the manuscript.

References

Aceñolaza, F.G., Miller, H., Toselli, A.J., 2002. Proterozoic–Early Paleozoic evolution in western South America: a discussion. Tectonophysics 354, 121–137.

Astini, R.A., Ramos, V.A., Benedetto, J.L., Vaccari, N.E., Cañas, F.L., 1996. La Precodillera: un terreno exótico a Gondwana. 13 Congreso Geológico Argentino y 3 Congreso de Exploración de Hidrocarburos. Actas, vol. 5, pp. 293–324. Buenos Aires.

Baldis, B.A., Peralta, S.H., 1999. Silúrico y Devónico de la Precordillera de Cuyo y Bloque de San Rafael. In: Caminos (Ed.), Geología Argentina. Instituto de Geología y Recursos Minerales-SEGEMAR. Anales, vol. 29 (10), pp. 215–238. Buenos Aires.

Baldo, E., Casquet, C., Rapela, C.W., Pankhurst, R.J., Galindo, C., Fanning, C.M., Saavedra, J., 2001. Ordovician metamorphism at the southwestern margin of Gondwana: P–T conditions and U–Pb SHRIMP ages from the Loma de Las Chacras, Sierras Pampeanas. Third South American Symposium of Isotope Geology, Pucón, Chile, SERNAGEOMIN, Santiago, pp. 544–547.

Bhatia, M.R., Crook, K.A.W., 1986. Trace element characteristics of graywackes and tectonic discrimination of sedimentary basins. Contributions to Mineralogy and Petrology 92, 181–193.

Bizzarro, M., Baker, J., Ulbeck, D., 2003. A new digestion and chemical separation technique for rapid and highly reproducible determination of Lu/Hf and Hf isotope ratios in geological materials by MC-ICP-MS. Geostandard Newsletters 27, 133–145.

Bodet, F., Scharer, U., 2000. Evolution of the SE-Asian continent from U–Pb and Hf isotopes in single grains of zircon and baddeleyite from large rivers. Geochimica et Cosmochimica Acta 64, 2067–2091.

Boso, M.A., Monaldi, C.R., 1999. La cuenca ferrífera del norte argentino, Jujuy y Salta. In: Zappettini (Ed.), Recursos Minerales de la República Argentina, Instituto de Geología y Recursos Minerales-SEGEMAR. Anales, vol. 35, pp. 529–544. Buenos Aires.

Casquet, C., Baldo, E., Pankhurst, R.J., Rapela, C.W., Galindo, C., Fanning, C.M., Saavedra, J., 2001. Involvement of the Argentine Precordillera Terrane in the Famatinian Mobile Belt: geochronological (U–Pb SHRIMP) and metamorphic evidence from the Sierra de Pie de Palo. Geology 29, 703–706.

Please cite this article as: Chernicoff, C.J. et al. Foreland basin deposits associated with Cuyania accretion in La Pampa Province, Argentina. Gondwana Research (2007), doi:10.1016/j.gr.2007.04.006

Chernicoff, C.J., Zappettini, E.O., 2003. Delimitación de los terrenos tectonoestratigráficos de la región centro-austral argentina: evidencias aeromagnéticas. Revista Geológica de Chile 30, 299–316.

Chernicoff, C.J., Zappettini, E.O., 2004a. Geophysical evidence for terrane boundaries in south-central Argentina. Gondwana Research 7, 1105–1116.

Chernicoff, C.J., Zappettini, E.O., 2004b. Foreland Basin deposits associated to the Cuyania terrane accretion in SW Gondwana, Argentina: a redefinition of the Carapacha Formation. 32 International Geological Congress. Florencia. Abstract.

Chernicoff, C.J., Zappettini, E.O., 2005a. Foreland basin deposits associated with Cuyania terrane accretion in La Pampa province, Argentina. Gondwana 12 Conference. Mendoza. Proceedings, p. 101.

Chernicoff, C.J., Zappettini, E.O., 2005b. Paleozoic foreland basin deposits (La Horqueta Formation) in the province of La Pampa, Argentina. 16 Congreso Geológico Argentino. Actas, vol. 2, pp. 169–176. La Plata.

Chernicoff, C.J., Zappettini, E.O., 2005c. Evidencias de una cuenca de *pull-apart* neopaleozoica en el sudeste de la provincia de San Luis, Argentina: extensión austral de la cuenca de Paganzo. 16 Congreso Geológico Argentino. Actas, vol. 1, pp. 471–476. La Plata.

Chernicoff, C.J., Zappettini, E.O., in press. La paleozoica de Arizona, sudeste de San Luis, Argentina: extensión austral de la cuenca de Paganzo. Revista de la Asociación Geológica Argentina 62.

Chernicoff, C.J., Zappettini, E.O, Villar, M.L., 2005. La faja de metagabros del sector centro-norte de la provincia de La Pampa, Argentina: nuevas evidencias geofisicas. 16 Congreso Geológico Argentino. Actas, vol. 3, pp. 39–44. La Plata.

Chernicoff, C.J., Zappettini, E.O., Villar, L.M., Chemale, F., Hernández, L., in press. The belt of metagabbros of La Pampa: Lower Paleozoic back-arc magmatism in south-central Argentina. Journal of South American Earth Sciences 23.

Chowns, T.M., 2002. Origin of sedimentary ironstones in the light of sequence stratigraphy of (Silurian) Birmingham iron ores, Alabama, USA. Geological Society of America, 2002 Denver Annual Meeting, Paper No. 89–7.

Cingolani, C.A., Monassero, M., Abre, P., 2003. Composition, provenance and tectonic setting of Ordovician siliciclastic rocks in the San Rafael block: southern extension of the Precordillera crustal fragment, Argentina. Journal of South American Earth Sciences 16, 91–106.

Cotter, E., Link, J.E., 1993. Deposition and diagenesis of Clinton ironstones (Silurian) in the Appalachian foreland basin of Pennsylvania. Geological Society of America Bulletin 105, 911–922.

Criado Roqué, P., 1972. Cinturón Movil Mendocino–Pampeano. In: Leanza, A. (Ed.), Primer Simposio de Geología Regional Argentina. Academia Nacional de Ciencias, Córdoba, pp. 287–295.

Dirección Nacional de Geología y Minería, 1958. Perfiles de perforaciones. Período 1904–1915. Dirección Nacional de Geología y Minería, Publicación No. 146, p. 175. Buenos Aires.

Espejo, P.M., Silva Nieto, D.G., 1985. Descripción geológica de las Hojas 34h, Puelches; 34i, Estancia La Unión (provincia de La Pampa) and 35h, Cerro Choique Mahuida; 35i, Pichi Mahuida (provincias de La Pampa y Río Negro). Dirección Nacional de Minería y Geología. Buenos Aires. Unpublished Report, pp. 1–30.

Espejo, P.M., Silva Nieto, D.G., 1996. Hoja Geológica 3966-II Puelches, 1:250.000. Dirección Nacional del Servicio Geológico. Buenos Aires. Boletín 216, 1–35.

Finney, S., Gleason, J., Gehrels, G., Peralta, S., Aceñolaza, G., 2003. Early Gondwanan connection for Argentina Precordillera terrane. Earth and Planetary Science Letters 205, 349–359.

Guerrak, S., 1988. Geology of the Early Devonian oolitic iron ore of the Gara Djebilet Field, Saharan Platform, Algeria. Ore Geology Reviews 3, 333–358.

Haïmeur, J., 1998. Lithostratigraphie, géochimie et métallogénie de l'environnement volcano-sédimentaire de l'amas sulfuré de Douar Lahjar (Guemassa, Maroc). Bulletin de l'Institut Scientifique 21, 15–30.

Hallam, A., Bradshaw, M.J., 1979. Bituminous shales and oolitic ironstones as indicators of transgressions and regressions. Journal of the Geological Society 136, 157–164.

Hartmann, L.A., Santos, J.O.S., 2004. Predominance of high Th/U, magmatic zircon in Brazilian Shield sandstones. Geology 32, 73–76.

Hartmann, L.A., Santos, J.O.S., Cingolani, C.C., McNaughton, N.J., 2002. Two Paleoproterozoic orogenies in the evolution of the Tandilia Belt, Buenos Aires, as evidenced by zircon U–Pb SHRIMP geochronology. International Geology Review 14, 528–543.

Hartmann, L.A., Bitencourt, M.F., Santos, J.O.S., McNaughton, N.J., Rivera, C.B., Betiollo, L., 2003. Prolonged Paleoproterozoic participation in the Neoproterozoic Dom Feliciano Belt, Santa Catarina, Brazil, based on zircon U–Pb SHRIMP geochronology. Journal of South American Earth Sciences 16, 477–492.

Kostadinoff, J., Llambías, E.J., 2002. Cuencas sedimentarias en el subsuelo de la provincia de La Pampa. 5 Congreso de Exploración y Desarrollo de Hidrocarburos. Actas. Artículo No. 49. Mar del Plata.

Leal, P.R., Hartmann, L.A., Santos, J.O.S., Miró, R., Ramos, V., 2003. Volcanismo postorogénico en el extreme norte de las Sierras Pampeanas Orientales: Nuevos datos geocronológicos y sus implicancias tectónicas. Revista Asociación Geológica Argentina 58, 593–607.

Linares, E., Llambías, E.J., Latorre, C.O., 1980. Geología de la provincia de La Pampa, República Argentina y geocronología de sus rocas metamórficas y eruptivas. Revista Asociación Geológica Argentina 35, 87–146.

Lopez Gamundi, O.R., Conaghan, P.J., Rossello, E.A., Cobbold, P.R., 1995. The Tunas Formation (Permian) in the Sierras Australes foldbelt, east central Argentina: evidence for syntectonic sedimentation in a foreland basin. Journal of South American Earth Sciences 8, 129–142.

Ludwig, K., 2001. Squid 1.02: A Users Manual. Berkeley Geochronology Centre. Special Publication, vol. 2. 19 pp.

Ludwig, K.R., 2003. Isoplot 3.00, a geochronological took-kit for Excel. Berkely Geochronology Center Special Publication, vol. 4. 67 pp.

Melchor, R.N., 1995. Sedimentología de las unidades paleozoicas aflorantes del centro-oeste de La Pampa, Argentina. Tesis Doctoral, Facultad de Ciencias Naturales y Museo, Universidad Nacional de La Plata, 272 pp. (unpublished).

Melchor, R.N., 1999. Redefinición estratigráfica de la Formación Carapacha (Pérmico), Provincia de La Pampa. Revista Asociación Geológica Argentina 54, 99–108.

Melchor, R.N., Césari, S.N., 1991. Algunos elementos paleoflorísticos de la Formación Carapacha (Pérmico inferior), Provincia de La Pampa, República Argentina. Ameghiniana 28, 247–352.

Melchor, R.N., Casadío, S., 1999. Hoja Geológica 3766-III La Reforma, Provincia de La Pampa. Servicio Geológico-Minero Argentino. Bulletin 295 (61 pp.).

McLennan, S.M., 1989. Rare earth elements in sedimentary rocks: influence of provenance and sedimentary processes. In: Lippin, B.R., McKay, G.A. (Eds.), Geochestry and Mineralogy of rare earth elements. Reviews in Mineralogy, vol. 21, pp. 169–200.

Pankhurst, R.J., Rapela, C.W., Fanning, C.M., Márquez, M., 2006. Gondwanide continental collision and the origin of Patagonia. Earth Science Reviews 76, 235–257.

Pearce, J.A., Harris, N.B.W., Tindle, A.G., 1984. Trace element discrimination diagrams for the tectonic interpretation of granitic rocks. Journal of Petrology 25, 956–983.

Porcher, C.C., Fernandes, L.A.D., Vujovich, G.I., Chernicoff, C.J., 2004. Thermobarometry, Sm/Nd Ages and Geophysical Evidence for the Location of the Suture Zone Between Cuyania and the Western Proto-Andean Margin of Gondwana. Gondwana Research 7, 1057–1076.

Ramos, V.A., 1984. Patagonia: ¿un continente a la deriva? 9 Congreso Geológico Argentino. Actas, vol. 2, pp. 311–325. Bariloche.

Ramos, V.A., 2000. The Southern Central Andes. In: Cordani, U.G., Milani, E.J., Thomaz Filho, A., Campos, D.A. (Eds.), Tectonic Evolution of South America. 31st Inter. Geol. Congress, Río de Janeiro, pp. 561–604.

Ramos, V.A., 2004. Cuyania, an exotic block to Gondwana: review of a historical success and the present problems. Gondwana Research 7, 1009–1026.

Rapela, C.W., Pankhurst, R.J., Casquet, C., Baldo, E., Saavedra, J., Galindo, C., Fanning, C.M., 1998. The Pampean orogeny of the southern proto-Andes: Cambrian continental collision in the Sierras de Córdoba. In: Pankhurst, R.J., Rapela, C.W. (Eds.), The Proto-Andean Margin of Gondwana. Special Publication of the Geological Society, London, vol. 142, pp. 181–217.

Rapela, C.W., Pankhurst, R.J., Baldo, E., Casquet, C., Galindo, C., Fanning, C.M., Saavedra, J., 2001. Ordovician metamorphism in the Sierras Pampeanas: New U–Pb SHRIMP ages in central-east Valle Fértil and the Velasco Batholith. Third South American Symposium of Isotope Geology, Pucón, Chile, SERNAGEOMIN, Santiago, pp. 616–619.

Rapela, C.W., Fanning, C.M., Pankhurst, R.J., 2005. The Río de la Plata Craton: the search for its full extent. Gondwana 12 Conference. Proceedings, p. 308.

Roser, B.P., Korsch, R.J., 1986. Determination of tectonic setting of sandstone–mudstone suites using SiO_2 content and K_2O/Na_2O ratio. Journal of Geology 94, 635–650.

Roser, B.P., Korsch, R.J., 1988. Provenance signatures of sandstone–mudstone suites determined using discriminant function analysis of major element data. Chemical Geology 67, 119–139.

Santos, J.O.S., 2003. Geotectônica dos escudos das Guianas e Brasil-Central. In: Bizzi, L.A., Schobbenhaus, C., Vidotti, R.M., Gonçalves, J.H. (Eds.), Geologia, tectônica e recursos minerais do Brasil, Companhia de Pesquisa de Recursos Minerais, Brasília, pp. 169–226. 674 pp.

Schieber, J., Riciputi, L., 2004. Pyrite ooids in Devonian shales record intermittent sea-level drop and shallow-water conditions. Geology 32, 305–308.

Schultz, C.J., 1986. Informe preliminar de la Formación Carapacha (Prov. de La Pampa). Actas 1° Jornadas de Biología y 2° Jornadas Geológicas de La Pampa. Univ. Nac. de La Pampa, Serie Suplementos No. 2: 29–36. Santa Rosa.

Tapia, A., 1939. Chacharramendi y alrededores. Physis, Revista de la Asociación Argentina de Ciencias Naturales, vol. 4, pp. 221–224 (Sección Geologia y Paleontología). Buenos Aires.

Terraza, J.C., 1981. Aspectos geológicos de la provincia de La Pampa. 1° Jornadas Geológicas de La Pampa. Univ. Nac. de La Pampa. Fascículo, vol. 1, pp. 1–18. Santa Rosa.

Terraza, J.C., Bazán, S., De Elorriaga, E., 1982. Geología del oeste de la Provincia de La Pampa. República Argentina. Resúmenes 5° Congreso Latinoamericano de Geología, pp. 24–25. BuenosAires.

Van Houten, F.B., Purucker, M.E., 1984. Glauconitic peloids and chamositic ooids — favorable factors, constraints, and problems. Earth-Science Reviews 20, 211–243.

Vavra, G., Schmid, R., Gebauer, D., 1999. Internal morphology, habit and U–Th–Pb microanalysis of amphibolite-to-granulite facies zircons: geochronology of the Ivrea Zone (Southern Alps). Contributions to Mineralogy and Petrology 134, 380–404.

Veevers, J.J., Belousova, E.A., Saeed, A., Sircombe, K., Cooper, A.F., Read, S.E., 2006. Pan-Gondwanaland detrital zircons from Australia analysed for Hf-isotopes and trace elements reflect an ice-covered Antarctic provenance of 700–500 Ma age, TDM of 2.0–1.0 Ga, and alkaline affinity. Earth-Science Reviews 76, 135–174.

Vilela, C.R., Riggi, J.C., 1956. Rasgos geológicos y petrográficos de la Sierra de Lihuél Calel y área circundante, provincia de La Pampa. Revista Asociación Geológica Argentina 11, 217–272.

Villar, L.M., Chernicoff, C.J., Zappettini, E.O., 2005. Evidence of a Famatinian continental magmatic arc at Paso del Bote, La Pampa province, Argentina. Gondwana 12 Conference. Proceedings, p. 365.

Vujovich, G.I., Fernandes, L.A.D., Ramos, V., 2004a. Cuyania: an exotic block to Gondwana — introduction. Gondwana Research 7, 1005–1007.

Vujovich, G.I., van Staal, C.R., Davis, W., 2004b. Age constrains on the tectonic evolution and provenance of the Pie de Palo Complex, Cuyania composite terrane, and the Famatinian orogeny in the sierra de Pie de Palo, San Juan, Argentina. Gondwana Research 7, 1041–1056.

Williams, L.B., Ferrell, R.E., 1991. Ammonium substitution in illite during maturation of organic matter. Clays and Clay Minerals 39, 400–408.

Zanettini, 1999. Los depósitos ferríferos de Sierra Grande, Río Negro. In: Zappettini (Ed.), Recursos Minerales de la República Argentina, IGRM-SEGEMAR. Anales, vol. 35, pp. 745–762. Buenos Aires.

Zappettini, E.O., Chernicoff, C.J., Villar, M.L., 2005. La faja de metagabros de La Pampa: evidencias geoquímicas y petrológicas de un magmatismo de retroarco en la región centro-austral argentina. 16 Congreso Geológico Argentino. Actas, vol. 3, pp. 45–52. La Plata.

Please cite this article as: Chernicoff, C.J. et al. Foreland basin deposits associated with Cuyania accretion in La Pampa Province, Argentina. Gondwana Research (2007), doi:10.1016/j.gr.2007.04.006